Developing a second nearest-neighbor modified embedded atom method interatomic potential for lithium

2012 Modelling Simul. Mater. Sci. Eng. 20 015014

(http://iopscience.iop.org/0965-0393/20/1/015014)

Modelling Simul. Mater. Sci. Eng. **20** (2012) 015014 (12pp) doi:10.1088/0965-0393/20/1/015014

Developing a second nearest-neighbor modified embedded atom method interatomic potential for lithium

Zhiwei Cui[1], Feng Gao[1], Zhihua Cui[2] and Jianmin Qu[1]

[1] Department of Civil and Environmental Engineering Northwestern University Evanston, IL 60208, USA
[2] Complex System and Computational Intelligence Laboratory Taiyuan University of Science and Technology Taiyuan, Shanxi Province, 030024, People's Republic of China

E-mail: j-qu@northwestern.edu

Received 2 August 2011, in final form 2 November 2011
Published 16 December 2011
Online at stacks.iop.org/MSMSE/20/015014

Abstract

This paper reports the development of a second nearest-neighbor modified embedded atom method (2NN MEAM) interatomic potential for lithium (Li). The 2NN MEAM potential contains 14 adjustable parameters. For a given set of these parameters, a number of physical properties of Li were predicted by molecular dynamics (MD) simulations. By fitting these MD predictions to their corresponding values from either experimental measurements or *ab initio* simulations, these adjustable parameters in the potential were optimized to yield an accurate and robust interatomic potential. The parameter optimization was carried out using the particle swarm optimization technique. Finally, the newly developed potential was validated by calculating a wide range of material properties of Li, such as thermal expansion, melting temperature, radial distribution function of liquid Li and the structural stability at finite temperature by simulating the disordered–ordered transition.

(Some figures may appear in colour only in the online journal)

1. Introduction

Lithium (Li) is an important element in industrial applications. For example, Li-based alloy is often used in coolants for heat transfer applications due to its high specific heat capacity [1]. In aerospace applications, Li is the best choice as an alloying element in aluminum (Al) because of its light weight. In addition to the reduction of density, some mechanical properties, such as Young's modulus and strength, have been enhanced with increasing Li concentration [2].

Atomistic simulations based on the molecular dynamics (MD) method have been widely used in recent years to understand and to model material behavior at small length scales. A critical element of MD simulations is the use of accurate and robust interatomic potential, which describes the interactions among atoms. One of the most widely used interatomic

potentials is the modified embedded atom method (MEAM) initially proposed by Baskes [3]. It has been used for a variety of materials including fcc, bcc and hcp metals, diamond and molecular materials with different degrees of success.

Recently, Lee *et al* [4] pointed out that the original MEAM interatomic potential has some drawbacks when used for studying the bcc crystal structures. For instance, the (1 1 1) surface energy was found to be smaller than that of (1 0 0) surface by the MEAM potential, which is contrary to experimental results or *ab initio* calculations. Also, the MEAM potential predicts that the most stable structure for Li at room temperature is not bcc, which is obviously incorrect. To better describe the bcc structure, Lee *et al* [4] proposed the second nearest-neighbor MEAM (2NN MEAM), and demonstrated that the 2NN MEAM provides a better potential of the bcc structure. Since then, 2NN MEAM potentials have been developed for several elements and their alloys including silicon [5] and magnesium [6].

In this paper, we report the development of a 2NN MEAM potential for Li using the particle swarm optimization [7–9] technique in conjunction with *ab initio* computations. The new 2NN MEAM potential is capable of not only predicting all the static properties of the reference system with good accuracy but also simulating the transition from a disordered state to an ordered state. Additionally, the new potential is also applicable to a wide range of structures with different coordination numbers. The accuracy of the new potential was validated by comparing the MD simulation results and the existing experimental data on several key physical properties.

The paper starts with brief introductions to the 2NN MEAM potential and the particle swarm optimization technique, followed by the optimization results. The newly developed potential is then validated by computing several key physical properties of Li and comparing the results with existing data.

2. Methodology

2.1. 2NN MEAM potential

In the 2NN MEAM formalism [4, 5], the total energy of a system is given by

$$E = \sum_i \left[F_i(\bar{\rho}_i) + \frac{1}{2} \sum_{j(\neq i)} \varphi_{ij}(R_{ij}) \right], \tag{1}$$

where F_i is the embedding function, $\bar{\rho}_i$ is the background electron density at site i, and $\varphi_{ij}(R_{ij})$ is the pair interaction between atoms i and j at a distance R_{ij}. The embedding function can be described by

$$F(\bar{\rho}) = AE_c(\bar{\rho}/\bar{\rho}^0)\ln(\bar{\rho}/\bar{\rho}^0), \tag{2}$$

where A is an adjustable parameter, E_c is the sublimation energy and $\bar{\rho}^0$ is the background electron density for a reference structure. Normally, the equilibrium structure is taken as the reference structure for elements. The background electron density $\bar{\rho}$ is composed of spherically symmetric partial electron density $\rho_i^{(0)}$ and angular contributions $\rho_i^{(1)}$, $\rho_i^{(2)}$ and $\rho_i^{(3)}$, which can be expressed as follows:

$$(\rho_i^{(0)})^2 = \left[\sum_{j\neq i} \rho_j^{a(0)}(R_{ij}) \right]^2, \tag{3}$$

$$(\rho_i^{(1)})^2 = \sum_\alpha \left[\sum_{j\neq i} (R_{ij}^\alpha / R_{ij}) \rho_j^{a(1)}(R_{ij}) \right]^2, \tag{4}$$

$$(\rho_i^{(2)})^2 = \sum_{\alpha,\beta}\left[\sum_{j\neq i}(R_{ij}^{\alpha}R_{ij}^{\beta}/R_{ij}^2)\rho_j^{a(2)}(R_{ij})\right]^2 - \frac{1}{3}\left[\sum_{j\neq i}\rho_j^{a(2)}(R_{ij})\right]^2, \tag{5}$$

$$(\rho_i^{(3)})^2 = \sum_{\alpha,\beta,\gamma}\left[\sum_{j\neq i}(R_{ij}^{\alpha}R_{ij}^{\beta}R_{ij}^{\gamma}/R_{ij}^3)\rho_j^{a(3)}(R_{ij})\right]^2 - \frac{3}{5}\sum_{\alpha}\left[\sum_{j\neq i}(R_{ij}^{\alpha}/R_{ij})\rho_j^{a(3)}(R_{ij})\right]^2. \tag{6}$$

Here $\rho_j^{a(h)}$ is the atomic electron densities of j atom at a distance R_{ij} relative to the site i and R_{ij}^{α} is the α component of the distance vector between atoms i and j. The total background electron density is then calculated as

$$\bar{\rho}_i = \rho_i^{(0)}G(\Gamma), \tag{7}$$

where

$$G(\Gamma) = 2/(1+\exp[-\Gamma]), \qquad \Gamma = \sum_{h=1}^{3} t_i^{(h)}[\rho_i^{(h)}/\rho_i^{(0)}]^2, \tag{8}$$

and $t_i^{(h)}$ is another adjustable parameter. The atomic electron density is given by

$$\rho_j^{a(h)}(R_{ij}) = \rho_0 \exp[-\beta^{(h)}(R_{ij}/r_e - 1)], \tag{9}$$

where ρ_0 is a scaling factor, $\beta^{(h)}$ are adjustable parameters and r_e is the nearest-neighbor distance in the reference structure after equilibrium. It has been found that the scaling factor ρ_0 has no effect in the case of pure elements, but plays a significant role in alloy system [4, 5].

In 2NN MEAM, the energy per atom in the reference structure is a function of nearest-neighbor distance R_{ij}, which can be extracted from a universal equation of state [10]

$$\begin{aligned} E^u(R) &= F[\bar{\rho}^0(R_{ij})] + \frac{1}{2}\sum\varphi(R_{ij}) \\ &= F[\bar{\rho}^0(R_{ij})] + (Z_1/2)\varphi(R_{ij}) + (Z_2S/2)\varphi(aR_{ij}) \\ &= -E_c[1+a^* + d(a^*)^3]e^{-a^*}, \end{aligned} \tag{10}$$

where

$$\bar{\rho}^0(R) = Z_1\bar{\rho}^{a(0)}(R) + Z_2S\bar{\rho}^{a(0)}(aR), \tag{11}$$

$$a^* = \alpha(R_{ij}/r_e - 1), \qquad \alpha = \sqrt{\frac{9B\Omega}{E_c}}. \tag{12}$$

In the above, $E^u(R)$ is the universal function to describe a uniform expansion or contraction in the reference structure, Z_1 is the number of first nearest-neighbor atoms, Z_2 is the number of second nearest-neighbor atoms, a is the ratio between the second and the first nearest-neighbor distances, S is the many-body screening factor, d is an adjustable parameter, B is the bulk modulus and Ω is the equilibrium atomic volume. Note that the many-body screening factor S is determined by two adjusting parameters, C_{max} and C_{min}, which are discussed in details in [5].

It is seen from the aforementioned equations that there are 14 parameters in the 2NN MEAM potential for a given material. These parameters are E_c, r_e, α, d, A, $\beta^{(0)}$, $\beta^{(1)}$, $\beta^{(2)}$, $\beta^{(3)}$, $t^{(1)}$, $t^{(2)}$, $t^{(3)}$, C_{max} and C_{min}. Among them, E_c and r_e are usually taken from experimental data. Therefore generally only 12 parameters are needed to be adjusted. For a given set of these parameters, a number of physical properties of Li, such as elastic constants and

surface energy, can be predicted by MD simulations. By fitting these MD predictions to their corresponding values from either experimental measurements or *ab initio* simulations, these adjustable parameters in the 2NN MEAM potential can be optimized to yield an accurate and hopefully robust interatomic potential for Li. In the next section, we will describe how such optimization was performed using the PSO technique.

2.2. Fitting procedures

In this work, we use the PSO method [7–9] to determine simultaneously all 14 parameters in the 2NN MEAM potential. The PSO method is a novel population-based optimization method. It was developed initially to simulate animal social behaviors, e.g., birds flocking, fish schooling and insects herding. Due to its simple algorithm and fast convergence, the PSO has been widely adopted in many areas such as power system [11], structural damage identification [12], nonlinear system identification [13] and ice-storage air-conditioning system [14].

The PSO method starts with a group (called swarm) of candidate solutions (called particles). These particles move around within the search space to seek food (called optimum). Let $\Pi(j)$ be an objective function that transforms a particle to a unique real number. The goal is to find a particular particle j such that $\Pi(j) \leqslant \Pi(k)$ for all particle k within the search space.

Let $\boldsymbol{x} = (x_1, x_1, \cdots x_M)$ represent a set of candidate parameters in the 2NN MEAM for a specific material. Thus the objective function for the optimization can be defined as

$$\Pi(\boldsymbol{x}) = \sum_{i=1}^{N} w_i \left[\frac{f_i(\boldsymbol{x})}{y_i} - 1 \right]^2, \tag{13}$$

where $f_i(\boldsymbol{x})$ is a physical property calculated by MD simulations using the 2NN MEAM potential with the parameter set $\boldsymbol{x}$. Such physical properties can be, for example, surface energy or elastic constant. The y_i is the corresponding value of the same physical property from either *ab initio* calculations or experimental measurements. The weighting factor w_i is a positive number selected based on the importance of this particular physical property. The objective here is to find an $\boldsymbol{x}$ so that $\Pi(\boldsymbol{x})$ is minimized for all $\boldsymbol{x}$ in the search space.

This is clearly a multi-parameter optimization problem. For efficiency, it is essential to define the bounds and weight factors for all the candidate parameters. The bounds used in this study are listed in table 1. These values are chosen based partially on previous results from other MEAM potentials and partially on the balance between accuracy and computational time. Deciding the weigh factors is somewhat subjective. In this study, structural properties are considered much more important than auxiliary structures, so they are given much larger weights.

To start the optimization, each parameter was assigned a random value within the defined bounds as the initial input. Physical properties of the Li systems were then computed based on the 2NN MEAM potential with this initial set of parameters. This gives the first iteration of $f_i(\boldsymbol{x})$ in (13). The next set of candidate parameters were then selected using the PSO algorithm. A small enough 'time step' was used in the PSO to ensure that each partial electron density term has the same order of magnitude. The above procedures were repeated until the objective function Π has been minimized below a predefined value ε, i.e. $\Pi(\boldsymbol{x}) < \varepsilon$. In this work, we used $\varepsilon = 0.05$.

The set of parameters that gives the minimum of Π are listed in table 1. For comparison purposes, the corresponding parameters used in the original MEAM potential for Li are also listed there. It is seen that some of the parameters remain unchanged, while others are quite different between these two potentials.

Table 1. Optimized parameters in the 2NN MEAM potential for Li, compared with those in MEAM by Baskes. The last column lists the bounds used during our optimization.

Parameters	MEAM [3] [Baskes]	MEAM [current]	Bounds
E_c	1.65	1.65	—
r_e	3.04	2.99	—
α	2.97	3.00	[3.0, 3.2]
d	0	0.14	[0.0, 0.2]
A	0.87	0.64	[0.0, 1.0]
$\beta^{(0)}$	1.43	1.03	[0.0, 10]
$\beta^{(1)}$	1.0	4.88	[0.0, 10]
$\beta^{(2)}$	1.0	4.15	[0.0, 10]
$\beta^{(3)}$	1.0	5.27	[0.0, 10]
$t^{(1)}$	0.26	−1.46	[−10, 10]
$t^{(2)}$	0.44	4.13	[−10, 10]
$t^{(3)}$	−0.20	−0.57	[−10, 10]
C_{max}	2.80	1.91	[1.0, 2.8]
C_{min}	2.00	0.31	[0.0, 0.5]

All the MD simulations in this study were conducted using the LAMMPS code [15, 16].

2.3. Database for fitting

As seen in (13), a database of physical properties y_i is needed in order to optimize the parameters in the 2NN MEAM for Li. In this work, the physical properties used include the elastic constants, unrelaxed surface energies and unrelaxed vacancy energy for the reference structure, as well as the binding energies of eight auxiliary structures, namely, five crystals (bcc, fcc, diamond, sc, hcp) and three molecular structures (Li_2, Li_3, Li_4). Among them, elastic constants and the unrelaxed surface energy were taken from experimental measurements in the open literature, and others were calculated by *ab initio* simulations.

The *ab initio* calculations were performed using the CASTEP software [17]. The ultrasoft pseudopotentials were used in conjunction with the Perdew–Burke–Ernzerhof generalized gradient approximations exchange correlation function. The k-mesh points in the Brillouin zone are $50 \times 50 \times 50$ for the largest reciprocal space and $20 \times 20 \times 20$ for the smallest reciprocal space by the Monkhorst–Pack scheme. The cutoff of plane-wave basis set is 500 eV/atom. The energy tolerance for the self-consistent field convergence is 5.0×10^{-7} eV/atom for all the calculations.

Examples of our *ab initio* calculation results are shown in figure 1, where the total energies (solids lines) of the auxiliary structures are plotted versus nearest-neighbor distance varying from 2.0 to 4.0 Å. Other physical properties from our *ab initio* calculations are listed in table 2.

3. Validation of the new 2NN MEAM potential for Li

3.1. Physical properties

Using the 2NN MEAM interatomic potential with the optimized parameters shown in table 1, we have computed several physical properties of Li. The results are listed in table 2. For comparison purpose, results from Baskes' MEAM potential are also listed in table 2. In comparison with the experimental data, the 2NN MEAM potential provides a better description of the phase transition energies, as well as the surface energies.

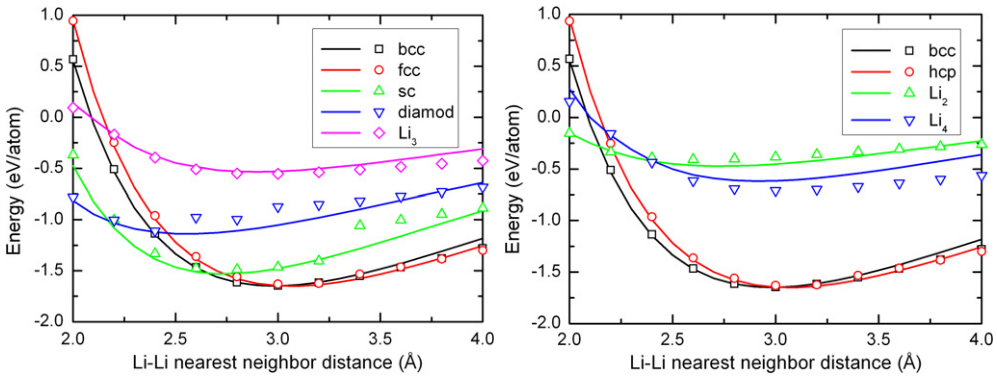

Figure 1. The comparison between the MD results (data points) and *ab initio* calculation (solid curve). Energies of several crystals and molecular structures are plotted versus the Li–Li nearest-neighbor distance.

Table 2. Physical properties of Li using various MEAM potentials.

Li		MEAM [27] [Yuan]	MEAM [3] [Baskes]	MEAM [Present]	Exp.	*ab initio*
C_{11} (GPa)		13.4	13.4	16.5	14.8 [28]	18.6
C_{12} (GPa)		11.3	11.3	11.0	12.5 [28]	11.3
C_{44} (GPa)		9.58	9.61	11.2	10.8 [28]	14.1
$\Delta E_{\mathrm{bcc}\to\mathrm{hcp}}$ (eV/atom)		0.022	−0.001	−0.012	−0.0016 [29]	−0.0015
$\Delta E_{\mathrm{bcc}\to\mathrm{fcc}}$ (eV/atom)		0.010	0.01	−0.012	−0.0011 [29]	−0.0015
E_v (eV)		0.495	0.34	0.66	0.52 [30]	
E_{surf} (erg cm^{-2})	(1 0 0)	535	431	424		467 [31]
	(1 1 0)	287	202	390		498 [31]
	(1 1 1)	463	279	537		560 [31]

Another comparison is made in figure 1, where the MD results based on the new 2NN MEAM potential are shown together with the *ab initio* calculation using the CASTEP software for the energies of eight auxiliary structures. Excellent agreement is seen between our MD and *ab initio* calculations.

An important validation of interatomic potentials for crystalline materials is to test their ability to simulate the transition from a disordered structure to an ordered structure. To this end, simulations were conducted using the 2NN MEAM potential to simulate the transition of Li from a disordered structure to a crystalline structure. The disordered structure was created by randomly displacing the atoms in an ordered structure by 1.0 Å from their original sites. Figure 2(*a*) shows such a disordered structure. The corresponding radial distribution function (RDF) is plotted on the side, which clearly indicates that the structure is indeed disordered. From this initially disordered structure, MD simulations were conducted to equilibrate the system. As the equilibration continues, the structure becomes more and more ordered and eventually fully recovers its original crystalline structure with identical cohesive energy and lattice constants. Figures 2(*b*)–(*d*) show several snapshots of the structure and its corresponding RDF during the equilibration. Such transition can be viewed as a special transition path from the molten state to a solid state.

It has been pointed out by Zhang *et al* [18, 19] that it is crucial for a robust interatomic potential to recover a disordered structure back to the practical equilibrium phase. Since the

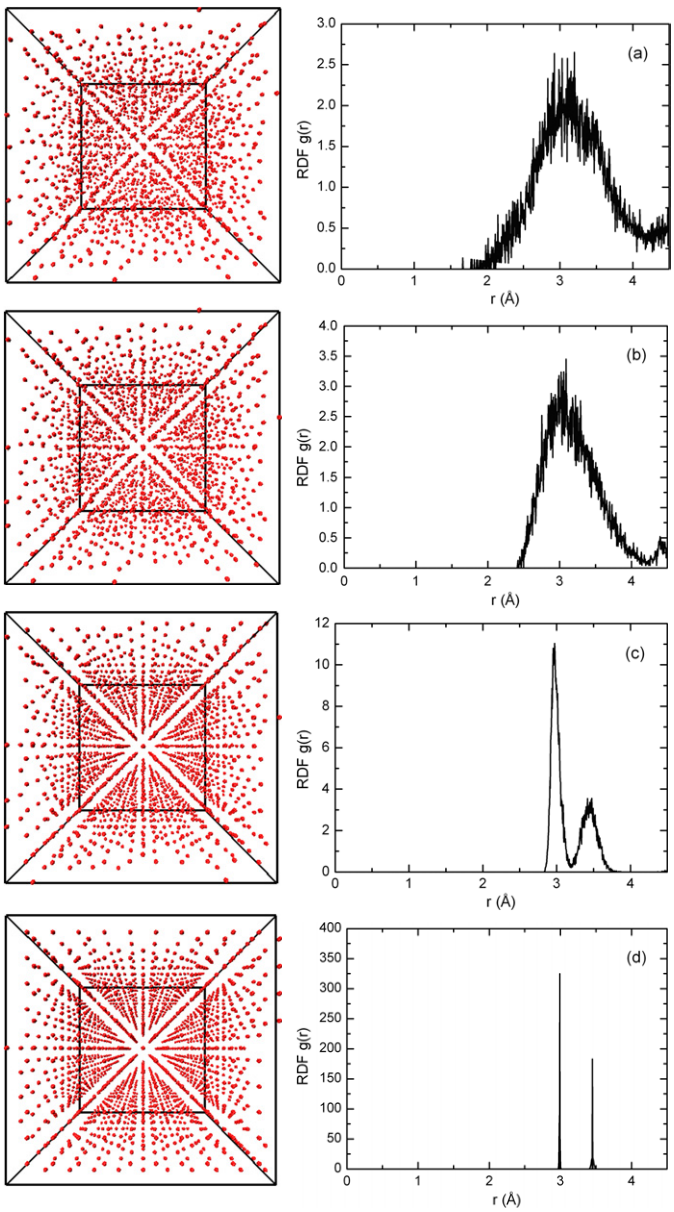

Figure 2. Several snapshots of intermediate structures and corresponding RDF during the transition from disordered (*a*) to ordered states (*d*).

disordered phase is constructed by randomly moving all atoms 1.0 Å from their equilibrium positions, successfully simulating the transition back to the originally order structure is an indication that the interatomic potential is valid over a wide range of interatomic distance. As a side note, we had also used the MEAM [3] potential for Li to conduct the same simulations. Our results seem to show that the MEAM [3] potential for Li is not capable of simulating this transition process. This is possibly the reason that the MEAM [3] potential does not predict stable bcc structure for Li at room temperature.

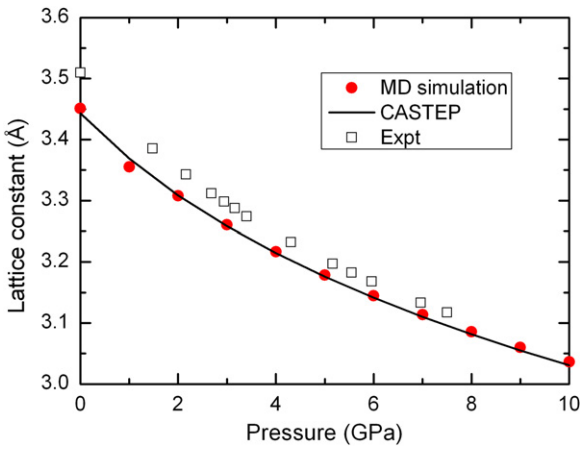

Figure 3. Calculated lattice constant as a function of applied pressure. The experimental results are from [20].

3.2. Deformation of BCC structure under high pressure at 0 K

To further validate the new 2NN MEAM potential, a Li bcc structure was subjected to an external pressure varying from 0 to 10 GPa. We want to see how the pressure changes the lattice structure. The comparison between our MD results and the *ab initio* results is shown in figure 3, as well as the experimental results. In the pressure range between 0 and 10 GPa, our MD results are in good agreement with the CASTEP calculations, while slightly lower than the experiment data [20]. This may be attributed to a larger lattice constant measured at room temperature in the experiment.

3.3. Thermal expansion

The newly developed 2NN MEAM interatomic potential was used to calculate the thermal expansion of Li. A $5 \times 5 \times 5$ bcc Li supercell (250 atoms) was constructed for the MD model with periodic boundary conditions (PBC) applied in all three perpendicular directions. MD simulations were then performed using the NPT ensemble. The cutoff distance used was 4.80 Å, which is between 2NN and 3NN distance. In each calculation, MD simulations were first run for 1000 ps to equilibrate the system. After that, an additional 2000 ps of simulations was run to record the structural changes at a certain temperature. The lattice constants were calculated between 0 and 450 K, as shown in figure 4. The experimental results [21, 22] are also presented in the figure for comparison. Based on the MD results, the coefficient of thermal expansion is $64 \times 10^{-6}\,\mathrm{K}^{-1}$ (0–100 °C), which is slightly larger than that of experiment data of $56 \times 10^{-6}\,\mathrm{K}^{-1}$ [23]. This is another piece of evidence that the new 2NN MEAM potential is valid.

3.4. Melting temperature and liquid Li

In this study, the melting temperature of element Li was estimated using an 'interface' model [24, 25]. In this model, the MD simulation box is composed of half solid Li and half liquid Li. At a given temperature, if after long enough equilibration time, the MD simulations predict only one stable phase, then the MD simulations will be re-run

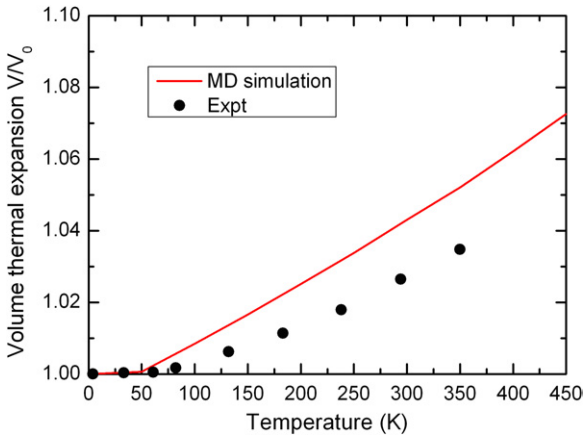

Figure 4. The thermal expansion of Li as a function of temperature. The experimental results are from [21, 22]

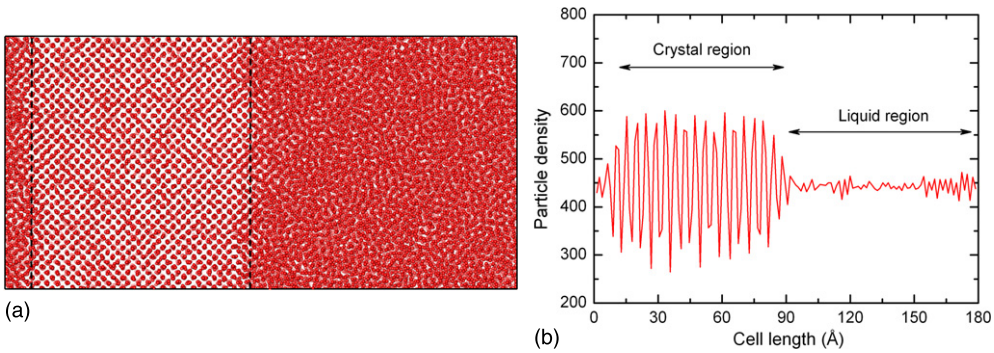

Figure 5. (*a*) A stabilized solid–liquid interface at the melting temperature; (*b*) the corresponding particle density distribution along the direction perpendicular to the solid–liquid interface. The vertical dashed lines indicate the solid–liquid interfaces after equilibrium.

with either a lower temperature if the single remaining phase is liquid, or with a higher temperature if the single remaining phase is solid. This trial-and-error calculation is repeated until a temperature is found, at which the MD simulations predict that both the liquid and solid phases can co-exist in a stable state for a sufficiently long time, without any appreciable trend towards melting or solidification. This temperature is considered the melting temperature.

In order to build such a solid–liquid interface model, two identical crystalline supercells (total 62500 atoms) of Li were created first. One of them was heated to 600 K to form a liquid and then subsequently cooled to 454 K, the experimentally measured melting temperature [23]. After that, this liquid Li supercell was juxtaposed to the solid crystal supercell. MD simulations were then performed under NVT and NPH ensembles in conjunction with PBC in all three perpendicular directions. At an appropriate temperature, the liquid–solid interface stabilized after 1000 ps. The average temperature of this stabilized interface system gives the melting point of Li. Using the 2NN MEAM potential, the melting temperature predicted using this approach 450 ± 10 K, which is consistent with the experiment data, 454 K from [23].

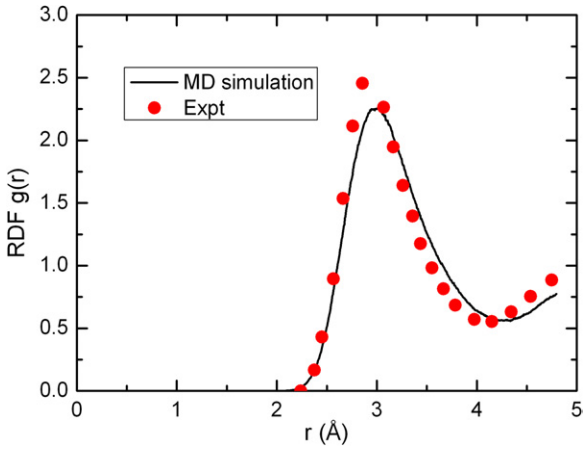

Figure 6. Comparison of RDF of liquid Li between MD simulations and experimental measurements. The experimental results are from [26].

A typical snapshot of the interface configuration predicted by the MD simulations at the melting temperature is shown in figure 5(*a*). The interface is located roughly at the center of the simulation cell. Due to the PBC used, the same interface can also be found at the left end of the simulation cell. The Li solid (crystal) phase is located between these two interfaces indicated by the dashed lines, while the rest is the liquid phase. Figure 5(*b*) shows the corresponding particle density of the interface system along the direction perpendicular to the interface. The higher and periodic profile of the particle density distribution function represents the domain of the crystal structure, while the lower and irregular density oscillating around a constant value is typically an indication of the liquid phase [25]. To further confirm the presence of liquid phase, the RDF of the right half of the simulation cell was then calculated. Figure 6 shows the comparison of the RDF between our MD simulations and experiment data [26]. It is seen that our MD results match well with the experimental measurements. In particular, the first peak of the RDF is found at 3.0 Å by MD simulation, which is in good agreement with the experimental data.

4. Summary and concluding remarks

In this paper, a methodology is proposed to derive the 2NN MEAM interatomic potential for the element Li based on the PSO technique. Using this methodology, a 2NN MEAM interatomic potential was developed for pure Li. To validate the new potential, several physical properties of Li were computed by MD simulations using the new potential. The MD results are then compared with data from either *ab initio* calculations conducted in this work or experimental measurements reported in the open literature. Excellent agreement is observed. In addition, we demonstrated that the new 2NN MEAM potential is more accurate and more robust than the existing MEAM potential for Li in that it applies to not only the basic bcc structure of Li but also the additional eight auxiliary structures, it is capable of predicting both the static properties and the stability of the crystal structure at finite temperatures by simulating the phase transition from disordered to ordered states.

Finally, we note that the methodology developed here can be extended to developing interatomic potentials for Li alloys such as Li–Si and Li–Mg etc. Results will be reported elsewhere.

Acknowledgments

This work was supported by ISEN Booster Award at Northwestern University. The authors also gratefully acknowledge the helpful discussions with Dr B-J Lee, Department of Materials Science and Engineering, Pohang University of Science and Technology, Republic of Korea.

References

[1] Hammond C R (ed) 2000 The elements *Handbook of Chemistry and Physics* (Boca Ration, FL: CRC press)
[2] Rioja R J 1998 Fabrication methods to manufacture isotropic Al–Li alloys and products for space and aerospace applications *Mater. Sci. Eng.* A **257** 100–7
[3] Baskes M I 1992 Modified embedded-atom potentials for cubic materials and impurities *Phys. Rev.* B **46** 2727–42
[4] Lee B J *et al* 2001 Second nearest-neighbor modified embedded atom method potentials for bcc transition metals *Phys. Rev.* B **64** 184102
[5] Lee B J 2007 A modified embedded atom method interatomic potential for silicon *Calphad* **31** 95–104
[6] Kim Y M, Kim N J and Lee B J 2009 Atomistic modeling of pure Mg and Mg-Al systems *Calphad* **33** 650–7
[7] Kennedy J and Eberhart R 1995 Particle swarm optimization *Proc. IEEE International Conf. on Neural Networks (Perth, WA, Australia)* vol 1–6, pp 1942–8
[8] Cui Z H and Zeng J C 2004 A guaranteed global convergence particle swarm optimizer *Rough Sets Curr. Trends Comput.* **3066** 762–7
[9] Cui Z H, Zeng J C and Sun G J 2006 A fast particle swarm optimization *Int. J. Innovative Comput. Inform. Control* **2** 1365–80
[10] Rose J H *et al* 1984 Universal features of the equation of state of metals *Phys. Rev.* B **29** 2963–9
[11] Vlachogiannis J G and Lee K Y 2009 Multi-objective based on parallel vector evaluated particle swarm optimization for optimal steady-state performance of power systems *Expert Syst. Appl.* **36** 10802–8
[12] Begambre O and Laier J E 2009 A hybrid particle swarm optimization simplex algorithm (PSOS) for structural damage identification *Adv. Eng. Softw.* **40** 883–91
[13] Chen S *et al* 2009 Non-linear system identification using particle swarm optimisation tuned radial basis function models *Int. J. Bio-Inspired Comput.* **1** 246–58
[14] Lee W S, Chen Y T and Wu T H 2009 Optimization for ice-storage air-conditioning system using particle swarm algorithm *Appl. Energy* **86** 1589–95
[15] http://lammps.sandia.gov
[16] Plimpton S 1995 Fast parallel algorithms for short-range molecular-dynamics *J. Comput. Phys.* **117** 1–19
[17] Clark S J 2005 *et al* First principles methods using CASTEP *Z. Kristallogr.* **220** 567–70
[18] Zhang S and Chen N X 2002 Ab initio interionic potentials for NaCl by multiple lattice inversion *Phys. Rev.* B **66** 064106
[19] Wang C, Zhang S and Chen N X 2005 Ab initio interionic potentials for CaO by multiple lattice inversion *J. Alloys Compounds* **388** 195–207
[20] Hanfland M *et al* 1999 Equation of state of lithium to 21 GPa *Solid State Commun.* **112** 123–7
[21] Anderson M S and Swenson C A 1985 Experimental equations of state for cesium and lithium metals to 20-Kbar and the high-pressure behavior of the alkali-metals *Phys. Rev.* B **31** 668–80
[22] Bhatt N K *et al* 2005 Thermodynamic properties of the alkali metals at high temperatures and high pressures using mean-field potential model *J. Phys. Chem. Solids* **66** 797–808
[23] Brandes E 1992 *Smithells Metals Reference Book*
[24] Timonova M and Thijsse B J 2011 Optimizing the MEAM potential for silicon *Modelling Simul. Mater. Sci. Eng.* **19** 015003
[25] Hernandez E R *et al* 2010 First-principles simulations of lithium melting: stability of the bcc phase close to melting *Phys. Rev. Lett.* **104** 185701
[26] Gonzalez D J, Gonzalez L E and Stott M J 2004 Surface structure of liquid Li and Na: An ab initio molecular dynamics study *Phys. Rev. Lett.* **92** 085501
[27] Yuan X Y *et al* 2003 Development of modified embedded atom method for a bcc metal: lithium *Modelling Simul. Mater. Sci. Eng.* **11** 447–56

[28] Simmons G and Wang H 1971 *Single Crystal Elastic Constants and Calculated Aggregate Properties: a Handbook* (Cambridge, MA: MIT Press)
[29] Saunders N, Miodownik A P and Dinsdale A T 1988 Metastable lattice stabilities for the elements *Calphad* **12** 351–74
[30] Derlet P M *et al* 1999 The embedded-atom model applied to vacancy formation in bulk aluminium and lithium *J. Phys.: Condens. Matter* **11** 3663–77
[31] Doll K, Harrison N M and Saunders V R 1999 A density functional study of lithium bulk and surfaces *J. Phys.: Condens. Matter* **11** 5007–19